A Field Evidence Model: How to Predict Transport in a Heterogeneous Aquifers at Low Investigation Level?

Alraune Zech[1][2], Peter Dietrich[1][3], Sabine Attinger[1][4], and Georg Teutsch[1]

[1]Helmholtz-Centre for Environmental Research - UFZ, Leipzig, Germany
[2]Utrecht University, Department of Earth Science, Utrecht, The Netherlands
[3]Eberhard Karls University Tübingen, Germany
[4]University of Potsdam, Germany

Correspondence: Alraune Zech (a.zech@uu.nl)

Abstract. Aquifer heterogeneity in combination with data scarcity is a major challenge for reliable solute transport prediction. Velocity fluctuations cause non-regular plume shapes with potentially long tailing and/or fast travelling mass fractions. High monitoring cost and presumably missing simple concepts have limited the incorporation of heterogeneity to many field transport models up to now.

5   We present a hierarchical aquifer model which combines large-scale deterministic structures and simple stochastic approaches. Such a heterogeneous conductivity can easily be integrated into a numerical models. Depending on the modelling aim, the required structural complexity can be adapted. The same holds for the amount of available field data. The conductivity model is constructed step-wise following field evidence from observations; though relying on as minimal data as possible. Starting point are deterministic blocks, derived from head profiles and pumping tests. Then, sub-scale heterogeneity in form of

10   random binary inclusions are introduced to each block. Structural parameters can be determined e.g. from flowmeter measurements.

As proof of concept, we implemented a predictive transport model for the heterogeneous MADE site. The proposed hierarchical aquifer structure reproduces the plume development of the MADE-1 transport experiment without calibration. Thus, classical ADE models are able to describe highly skewed tracer plumes by incorporating deterministic contrasts and effects of connectivity in a stochastic way even without using uni-modal heterogeneity models with high variances. The reliance of

15   the conceptual model on few observations makes it appealing for a goal-oriented site specific transport analysis of less well investigated heterogeneous sites.

1 Introduction

20 Groundwater is extensively used worldwide as the major drinking water resource and consequently needs to be protected with respect to quantity and quality. Increasing pressure on the quality originates from the intensification of agriculture using agrochemicals (non-point sources), an increased urbanization with the resulting solid and liquid wastes and contaminant spills from industrial applications (point sources).

Essential for groundwater protection is the quantitative analysis of the fate and transport of various contaminants in the
25 groundwater body. This can be either for a provisional risk assessment or for the clean-up of an already existing groundwater contamination. Numerical models are common tools to quantify the flow and transport, where partial differential equations are solved using initial and boundary conditions (Bear, 1972; Fetter, 2000).

For simplicity, we restrict ourselves to saturated flow and transport of a dissolved, non-reactive contaminant. The governing equation for its concentration $C(x,t)$ is the advection-dispersion equation (ADE) (Bear, 1972):

$$30 \quad \frac{\partial C(x,t)}{\partial t} = -u(x,t) \cdot \frac{\partial C(x,t)}{\partial x} + \frac{\partial}{\partial x}\left(D \cdot \frac{\partial C(x,t)}{\partial x}\right) \tag{1}$$

given here in one spatial dimension x and time t. D is the macro-dispersion coefficient and $u(x,t)$ is the Darcy velocity. The latter is a function of the hydraulic gradient J and the heterogeneous hydraulic conductivity $K(x)$ through Darcy's Law. A proper description of the velocity field $u(x,t)$ is crucial for predicting the concentration distribution $C(x,t)$.

The adequate parametrization of the heterogeneous conductivity $K(x)$ poses a significant challenge in practical model
35 development due to the lack of data. Numerous deterministic and stochastic approaches have been developed to incorporate the effects of spatial heterogeneity of conductivity on flow and transport, particularly in the context of stochastic subsurface hydrology (Dagan, 1989; Gelhar, 1993; Koltermann and Gorelick, 1996). On one hand, fully deterministic approaches use either uniform (effective) conductivities in large domains or maps of heterogeneity, created by interpolation, e.g. Kriging (Kitanidis, 2008). The former approach requires only few data to the price of neglecting local effects of heterogeneity. The
40 latter requires a huge amount of observation data which is hardly ever available in practical cases. Furthermore, conductivity fields from interpolation result in smooth structures lacking geological realism. On the other hand, stochastic methods allow to resolve heterogeneity based on a limited amount of data. Thus, they are able to capture the uncertainty in flow and transport predictions caused by heterogeneity. Common methods as (i) Gaussian random fields (Freeze, 1975; Dagan, 1989; Gelhar, 1993; Zinn and Harvey, 2003); (ii) indicator/hydrofacies models (Carle and Fogg, 1996; Fogg et al., 2000); or (iii) multi-point
45 statistics/training images (Renard et al., 2011; Linde et al., 2015) allow to create spatially distributed conductivity fields of higher geological realism. Modelling flow and transport in ensembles of heterogeneous fields (Monte Carlo approach) do not only provide mean behavior but also uncertainty ranges.

Log-normal random fields require a number of parameters like geometric mean, log-variance and spatial correlation lengths in horizontal and vertical directions. They result from geostatistical analysis of spatially distributed observations, e.g. from
50 flowmeter, permeameter or injection logging, as DPIL (Dietrich et al., 2008). Despite increased efficiency in exploration methods, the cost and effort related to gather sufficient data hampers the application in practice. Alternatively, hydrofacies models use indicator geostatistics with transition probability to generate geological heterogeneity structures. Although conceptually

different, the general amount of input data is similarly high. Training images are known for their geological realism, but depend strongly on the high resolution input data, e.g. reconstructed images from outcrop studies. Not only the availability of a training

55 image limits their application, but particularly the question if it is representative for the larger aquifer domain where transport is modeled (Koltermann and Gorelick, 1996).

A recent debates series (Rajaram, 2016; Fiori et al., 2016; Fogg and Zhang, 2016; Cirpka and Valocchi, 2016; Sanchez-Vila and Fernàndez-Garcia, 2016) outlined the gap between the advanced research in stochastic subsurface hydrology and its application in the practice of groundwater flow and transport modeling. We see a significant reason in the lack of data for

60 complex stochastic models. Thus, we propose a novel approach which focuses on optimizing the available field data adaptive to the simulation target. Thereby, we aim to provide a tool making aquifer heterogeneity more accessible for practical applications.

Our approach is based on the fact that subsurface heterogeneity can be generally classified into

    a) larger scale dominant features which primarily determine the general flow direction together with the average groundwater flow velocity; and

65   b) smaller scale features which are responsible for the dispersion, respectively the spatial spreading of a contaminant or solute.

We create a deliberate connection between the model parameterization requirements and the field characterization methods employed for measurement. Pumping tests, for example, are a recommended characterization method to determine the spatially averaged transmissivity respectively hydraulic conductivity, even in a heterogeneous aquifer environment (Zech et al., 2016).

70 Together with the averaged gradient estimated from piezometric levels this yields good estimates of the mean groundwater flow velocities. On the other hand, high resolution, small-scale borehole logs of hydraulic conductivity (e.g. from flowmeter or DPIL) can provide the data needed to estimate the variability of the hydraulic conductivity field and consequently the dispersion parameters needed.

We demonstrate the methodology using field characterization data from MADE, a heterogeneous, well investigated research

75 field site (e.g. Boggs et al. (1990); Zheng et al. (2011); Gomez-Hernandez et al. (2017)). Following our adaptive approach, we use a minimum of field data on aquifer properties to construct a numerical transport model and to predict tracer plume behavior following a Monte Carlo approach. Predictions are independently evaluated using field tracer data from the MADE-1 experiment (Boggs et al., 1992). They shows good agreement also compared to other complex predictive transport models for MADE (e.g. Fiori et al. (2013, 2017)).

80 The course of the paper is the following: section 2 features the approach in light of different modeling aims. Section 3 is dedicated to the application of the methodology for the MADE aquifer. We close with a summary and conclusions in section 4.

2 Approach

Large scale hydraulic structures of hundreds or more meters determine the groundwater flow direction and magnitude in combination with groundwater catchment boundaries. Subsequently, they set the mean transport velocity. This is the key

Hydrology and
Earth System
Sciences
Discussions

85 parameter to predict the location of the bulk mass of substances dissolved in the groundwater when input conditions are known.

Variations of hydraulic properties on intermediate scale, in the range of tens of meters, generate spatially variable flow fields. They also render transport velocities variable at these scales resulting in a larger spreading of plumes. This is particularly important for modeling tailing or leading mass fronts. Fluctuations on scales smaller than these intermediate scales have a

90 blending effect, generally increasing local mixing and macro-dispersion (Werth et al., 2006).

Following this conceptual view, we generate hydraulic conductivity fields composed of three components: Module (A), (B) and (C) which capture the effects at large, intermediate and small scale heterogeneity, respectively. Each component is selected according to the model aim and the data at hand to parametrize the hydraulic conductivity for this component.

The procedure is exemplified for the MADE site. This significantly heterogeneous site was intensively investigated with

95 various measurement devices providing many different data sets, as pumping tests, flowmeter and DPIL measurements (Boggs et al., 1990; Bohling et al., 2016). Detailed information on MADE can be found in section 3 and the *Supporting Information*.

In the approach, we considers several steps:

1. Specifying the aim of the model: What do we want to predict?

2. Selecting processes and process components which need to be accounted for in the model: What does this imply for the
100   conceptualization of hydraulic conductivity?

3. Selecting suitable measurement methods: Which method can deliver the data needed for parameterizing hydraulic conductivity with minimal effort?

4. Conceptualizing hydraulic conductivity.

5. Calculating flow and transport.

105 Before specifying the hydraulic conductivity component Modules (A), (B) and (C), we illustrate our concept discussing two exemplary model aims.

2.1 Exemplary Model Aims

Model Aim "Mean Arrival"

1. **Aim**: Prediction of mean arrival of a contaminant from a point source.

110 2. **Processes:** Estimation of regional groundwater movement, direction and magnitude of flow making use of the groundwater flow equation and Darcy's law. Transport is modelled by advection. For sake of simplicity we do not consider reactivity.

3. **Field characterization:** Regionalized groundwater level measurements provide direction and magnitude of hydraulic gradient. It is critical to outline areas of different gradients (zones) indicating regional hydraulic conductivity trends and
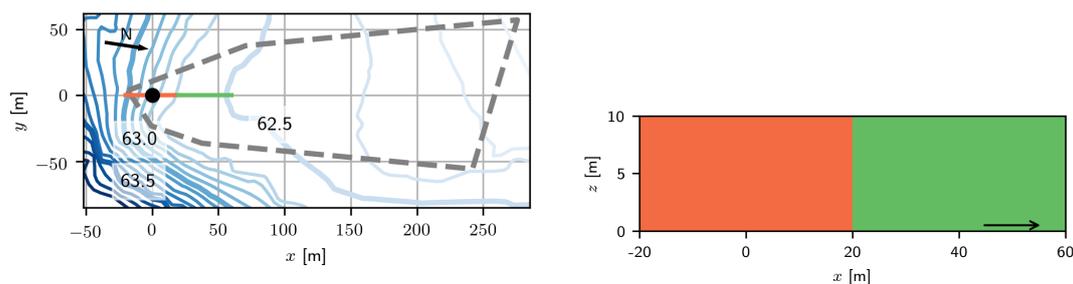
Figure 1. Left: Potentiometric surface map of head measurements according to Boggs et al. (1990). Orange-Green line indicates location of cross section displayed right: Concept (Module A) for large conductivity structure with deterministic zones of low (orange) and high (green) conductivity. Arrow indicates flow direction.

115   large scale heterogeneity. Pumping tests can provide independent values of effective transmissivity within each zone (Kruseman and de Ridder, 2000).

4. **Conceptualization of hydraulic conductivity:** Conductivity is considered homogeneous within each large scale zone. Effects of heterogeneity are captured in effective parameters representing average flow behavior, e.g. determined from pumping tests.

120   5. **Solving flow and transport:** Flow is solved either analytically, e.g. for one or two zones of different effective hydraulic conductivity, or numerically in case of a more complex spatial distribution of zones. Transport can be determined making use of analytical or numerically solutions of the ADE according to initial and boundary conditions.

2.1.1 Example MADE

The piezometric surface map of MADE (Boggs et al., 1992, Fig. 3) shows a significant non-uniform hydraulic head pattern.
125   The reproduced head contours in Figure 1a allow to delineate two major zones: an area of low conductivity upstream (left) and high conductivity downstream (right). Two large scale pumping tests confirm the contrast in mean conductivity of about two orders of magnitude (Boggs et al., 1992). Consequently, flow should be modelled with distinct mean conductivity in two vertical zones (Figure 1b) when aiming to model mean arrival times for the MADE site.

Model Aim "Risk Assessment"

130   1. **Aim:** Prediction of early or late arrival of contaminants commonly used in risk assessments.

2. **Processes:** Flow and transport equations; it is particularly relevant to capture variability in transport velocity to estimate spreading behavior of plumes.
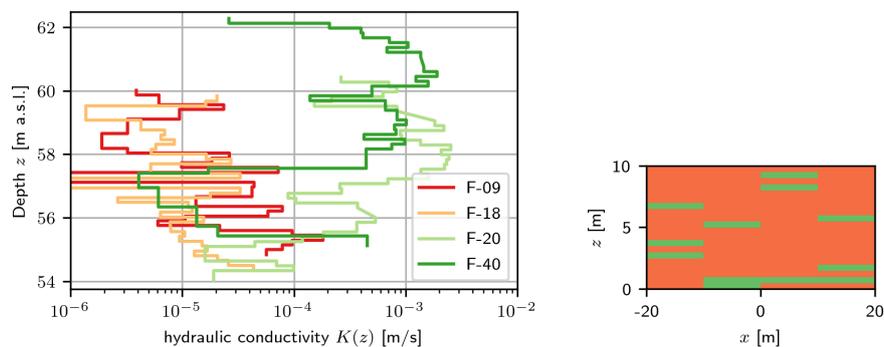
Figure 2. Left: Four flowmeter logs of hydraulic conductivity $K(z)$ versus depth z; the logs *F-09* and *F-18* are close to the tracer test injection location; *F-20* and *F-40* are several tenth of meters downstream (see Figure 3). Right: Concept of binary inclusion structure (Module B) with 15% high conductivity inclusions (green) embedded in the bulk of low conductivity (orange).

3. **Field characterization:** Detecting and delineating high and low conductivity subsurface structures with a characteristic horizontal length scale of several meters. Typical examples are channels formed in braided river systems. Typical investigation methods giving field evidence of such heterogeneity structures are small scale slug tests, borehole flowmeter logs or permeameter tests detecting strongly vertically varying conductivity.

4. **Conceptualization of hydraulic conductivity:** Spatially structured non-uniform conductivity.

5. **Solving flow and transport:** Small variations in conductivity allow to apply analytical solutions with effective measures, e.g. from first order theory (Dagan, 1989). Spatially resolved heterogeneity requires numerical solution of flow and transport with numerical tools (Monte Carlo approach).

2.1.2 Example MADE

Borehole flowmeter logs at MADE (Rehfeldt et al., 1989; Boggs et al., 1990) reveal horizontal layers with conductivity differences over $2 - 3$ orders of magnitude. For instance, the flowmeter log *F-40* shown in Figure 2a has a bulk of high conductivity values with about 15% of values being two orders of magnitude smaller. Logs at other locations (*F-09* and *F-18*) show the inverse behavior: a bulk of low conductivity values with embeddings of high conductivity.

Such strong vertical variation indicate the presence of high conductivity channels acting as preferential flow path and low conductivity zones with stagnant flow which both impact strongly on plume spreading behavior. Consequently, when aiming to model early and late plume arrival these feature need to be accounted for in a flow and transport model for the MADE site.

2.2 Scale-dependent Conductivity Modules

150 Given the scale-dependency of hydraulic conductivity features and their distinct relevance for flow and transport predictions, we propose three components: Module (A), (B) and (C) which capture large, intermediate and small scale heterogeneity effects, respectively. Given a certain model aim, components are selected (or not) with regard to the available field data. We shortly discuss the Modules and motivate their use based on the data of the MADE site example for different aims.

Module A

155 The aquifer domain of interest is divided into deterministic zones of significantly different mean conductivity (i.e. more than one order of magnitude). The structure can comprise horizontal or vertical layering simply in blocks or complex zone geometries depending on information available.

The zones represent large scale geological structures exhibiting conductivity differences potentially over several orders of magnitude as a results of changes in deposition history or changes in the material's composition (Bear, 1972; Gelhar, 1993).

160 Zones can be delineated using geologic maps, piezometric surface maps and geophysical methods providing information on aquifer structure, sedimentology and genesis. Pumping tests are suitable for identifying mean conductivities for each zone due to their large detection scale. Flow simulations on the deterministic zone structure should reproduce the observed head pattern.

The MADE site is an example where the concept of two zones of different mean hydraulic conducitivity (Figure 1b) can reprocude conceptually the hydraulic head pattern. Details will be discussed in section 3.
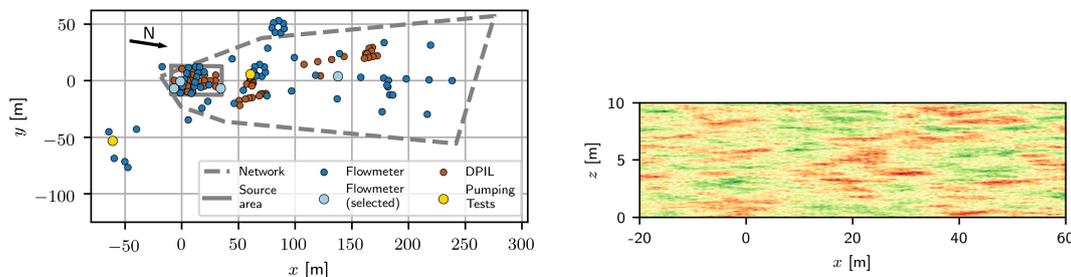
Module B

165

When hydraulic conductivity shows heterogeneous features at the same length scale as the plume transport itself, they require proper resolution. A contaminant plume typically passes several of these intermediate scale features but not enough to ensure ergodic transport behavior. Thus, using effective parameters is not warranted. Since limited data availability precludes from a deterministic representation of these features, stochastic approaches suit best.

170 Binary stochastic models are the simplest way to capture the effects of intermediate scale features. Figure 2b shows an example how to conceptualize a medium with two K values: inclusions (K_2) are embedded in the bulk conductivity (K_1), with p characterizing the percentage of K_2. Inclusions of high conductivity may represent preferential flow paths whereas inclusions of low conductivity can be obstacles like clay lenses.

The inclusion topology is a matter of choice and data availability. A simple design is a distribution of non-overlapping

175 blocks with horizontal length I_h and thickness I_v as in Figure 2b with $p = 15\%$, $I_h = 5\,\mathrm{m}$ and $I_v = 0.5 - 1\,\mathrm{m}$. More complex layering structures can be adapted if additional topological information is available. However, the specific topology often plays a subordinate role. When not having any information on spatial correlation of heterogeneity, it is beneficial to assume some instead of sticking to a homogeneous model.

Characteristic length scales in vertical direction I_v are detectable with low effort from a few borehole logs (Figure 2a).

180 Characteristic horizontal length as I_h are critical since they require spatially distributed observations. A parametric uncertainty

Figure 3. Left: Locations of measurements and tracer test observation network according to Boggs et al. (1990); Bohling et al. (2016). Right: Gaussian random field with exponential co-variance structure as conceptual module for small scale conductivity (Module C).

approach can keep the effort low. A range of reasonable I_h values is estimated (e.g. using expert knowledge) and applied in the random inclusion model. A sensitivity analysis reveals the impact of the parametric uncertainty of I_h on transport results.

The binary structure as in Figure 2b is beneficial in its plain stochastic concept relying on few input data, simple implementation and low computational requirement. It can be combined with Module (A) by implementing it within every deterministic

185   zone preserving the mean conductivities. As for MADE, the inclusions represent the contrasting vertical layers as observed in flowmeter logs (Figure 2a), from which the inclusion parameters can be deduced for every deterministic zone (section 3).

Module C

Variations in grain size and soil texture form small scale heterogeneities of characteristic length scales up to one meter. Their relevance for transport predictions depends on ergodicity and thus, on the degree of heterogeneity. Ergodicity is usually assumed

190   when the plume has traveled $10 - 100$ characteristic lengths. Then, effective parameters can capture effects of heterogeneity. Otherwise, the use of a spatial random representation is warranted.

If required, small scale features can be conceptualized with a log-normal conductivity distribution $K(\boldsymbol{x}) \propto \mathcal{LN}(K_{\mathrm{G}}, \sigma_Y^2)$ with geometric mean K_{G} and log-variance σ_Y^2. Including a spatial correlation structure depends on the acquired complexity and the availability of two-point statistical data as correlation length and anisotropy. Figure 3b gives an example.

195   Geostatistical parameters can be inferred from spatially distributed observations (Figure 3a), e.g. permeameters, borehole flowmeter, or injection logging (Figure 4). This is related to high effort and costs. Novel techniques like DPIL (Dietrich et al., 2008; Bohling et al., 2016) can provide a large amount of data at acceptable costs and time, but they are only accessible for shallow sites. Alternatives can be approaches which derive geostatistical parameters directly from pumping tests (Zech and Attinger, 2015; Zech et al., 2016) or dipole tracer test (Zech et al., 2018).

200   When combining with larger heterogeneity structures, small scale fluctuations are subordinate. In case of field evidence, Module (C) can be combined with Modules (A) and (B) by adding zero-mean fluctuations. According to Lu and Zhang (2002), the variances of heterogeneous sub-structures is additive. Thus, the log-normal variance relates to a 'variance gap' between the total variance, e.g. from a geostatistical analysis of the entire domain, and the binary model's variance (Module B). It can
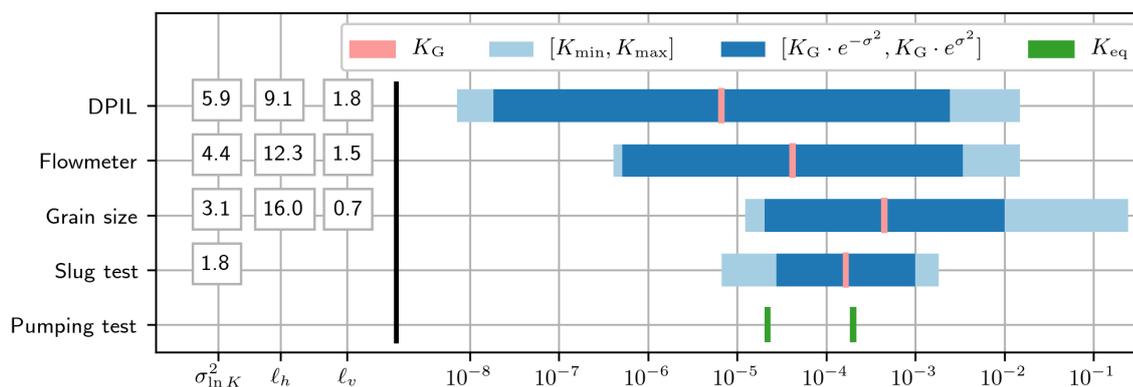
Figure 4. Geostatistical measures for MADE from DPIL (direct push injection logging) (Bohling et al., 2016), flowmeter, grain size analysis, slug tests (Rehfeldt et al., 1992) and effective mean values (K_{eff}) of two large scale pumping tests (Boggs et al., 1990): log-conductivity variance $\sigma_{\ln K}^2$, horizontal and vertical correlation length ℓ_h and ℓ_v, respectively. Visualization of range of observed values from minimal ($K_{\min}$) to maximal ($K_{\max}$), variance range and geometric mean K_{G}.

be interpreted as the system's variance which is not captured by intermediate and large scale heterogeneity. The length scales

205 for a correlation structure should be significantly smaller than the inclusion lengths of Module (B). Including small-scale heterogeneity enhances the realism of conductivity structure – however, on the expanse of increasing investigation costs.

The MADE site is a rare example with geostatistics from multiple observation methods (Figures 3a and 4). Methods well suited for small scale heterogeneity show large variances from 4.5 up to 5.9. Given the high variance and the low mean conductivity, ergodic conditions cannot be assumed for transport within the range of a few hundred meters.

210 The large value in variance, as determined for MADE, can likely be the result of preferential flow and/or trends in mean conductivity. Thus, explicitly representing deterministic zones (Module A) and preferential flow paths (Module B) might render the representation of small scale features (Module C) redundant. Modeling hydraulic conductivity as log-normal fields solely based on Module (C) seems warranted when there is no indication for deterministic zones or preferential pathways.

3 Predictive Transport Model for MADE

215 We validate our approach by performing flow and transport calculation for the MADE setting. Based on the scale-dependent conductivity modules (section 2.2), we derive different conductivity structures according to the field evidence given the structural data at MADE. The computed tracer plume is compared to the MADE-1 transport experiment (Boggs et al., 1992; Adams and Gelhar, 1992).

Following the approach steps outlined in section 2, we define our model aim broader then specified in section 2.1: The target

220 is predicting the general plume behavior. This might serve different purposes as e.g remediation and includes the mean flow behavior. The fact that there is no break-through curve data available for MADE, inhibits to study the subject of arrival times.

Particularly critical is first arrival as discussed in Adams and Gelhar (1992). Processes involved here are flow and transport governed by Darcy's Law and the Advection-Dispersion-Equation (Eq. 1).

3.1 MADE Field Data

225 The MADE site is located on the Columbus Air Force Base in Mississippi, U.S.A. The aquifer was characterized as shallow, unconfined, about $10 - 11$ m thick with a porosity of 0.32 (Boggs et al., 1992). It consists of alluvial terrace deposits composed of poorly sorted to well-sorted sandy gravel and gravely sand with significant amounts of silt and clay. The first extensive field campaign by Boggs et al. (1990) yielded a multitude of hydro-geological information, as e.g. piezometric surface maps and hydraulic conductivity observations from soil samples, flowmeter and pumping tests (Figure 4). Field campaigns in subsequent
230 years supplemented observations and data interpretations. For an overview see e.g. Zheng et al. (2011); Bohling et al. (2016) or Table 1 in the *Supporting Information*.

The MADE-1 transport experiment was conducted in the years 1986–1988 (Boggs et al., 1990, 1992; Rehfeldt et al., 1992; Adams and Gelhar, 1992). A pulse of bromide was injected over a period of $48.5h$ applying a flow rate of 3.5 l/min. The forced input conditions enlarged the tracer body at the source. Transport then took place under ambient flow conditions.

235 Concentrations were observed within a spatially dense monitoring network at several times after injection. We focus on the reported longitudinal mass distribution of Adams and Gelhar (1992, Fig.7) at six times: 49, 126, 202, 279, 370, and 503 days after injection. Values are integrated measures over transverse planes and accumulated over slices of 10 m length, given at the centers of slices at -5 m, 5 m, 15 m, …. The reported mass does not display mass recovery except at 126 days with recovery rates of $2.06, 0.99, 0.68, 0.62, 0.54$, and 0.43, for the six times, respectively. We do not normalize the reported mass to
240 recovered mass, but stick to the actually observed values associating the mass loss to insufficient sampling in the downstream zone as discussed in details by Fiori (2014).

3.2 Hydraulic Conductivity Structures

Three hydraulic conductivity conceptualizations are designed in line with the specifications for MADE in section 2, which serve different model aims. Modules (A), (B) and (C) are combined successively to capture the scale hierarchy of heterogeneity at
245 the MADE site. Figure 5 illustrated examples for each conceptualization.

3.2.1 Deterministic Zones (A)

As indicted by the piezometric surface map (Figure 1), we chose two vertically arranged deterministic zones (Figure 5): a low in average conductivity zone Z_1 from upstream of the tracer input location to $x = 20$ m downstream and zone Z_2 as high-in-the-average conductivity area from 20 m downstream of the source. We fix average conductivity values of $\bar{K}_{Z1} = 2e - 6$ m/s
250 and $\bar{K}_{Z2} = 2e - 4$ m/s with a contrast of two orders of magnitude as stated by Boggs et al. (1992). The specific values are chosen according to the two large scale pumping test (Boggs et al., 1992) and the head level rise during injection which is particularly important for early plume development. Details are given in the *Supporting Information*. This deterministic
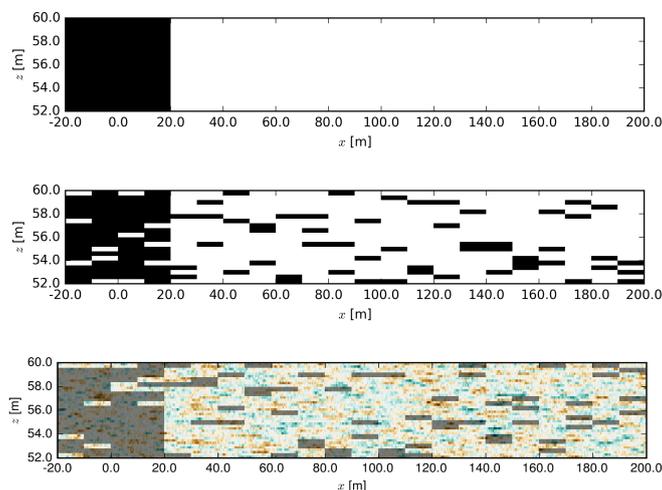
Figure 5. Realizations of hydraulic conductivity structures: (top) Deterministic zones (Module A), low K_1 in black, high K_2 in white. (center) Inclusions in deterministic zones (Modules A+B); amount of inclusions $p = 15\%$, inclusion lengths $I_h = 10\,\mathrm{m}$, $I_v = 0.5\,\mathrm{m}$. (bottom) Inclusions in deterministic zones and sub-scale heterogeneity (Modules A+B+C); correlation lengths $\lambda_h = 2.5\,\mathrm{m}$, $\lambda_v = 0.125\,\mathrm{m}$.

conductivity conceptualization is suitable for properly modelling the regional groundwater in line with the model aim "Mean Arrivel" as specified in section 2.1.

3.2.2 Inclusion Structure in Zones (A+B)

Flowmeter logs from MADE show a significant discontinuous heterogeneity in the layering (Figure 2). We represent these structures making use of the simple binary inclusion structured described in section 2.2.

The binary conductivity distribution is constructed for the entire domain comprising both deterministic zones. The upstream zone Z_1 consists of a bulk of low conductivity K_1 with a percentage p of high conductivity K_2 inclusions; the downstream zone Z_2 vice versa (Figure 5).

We identify the specific values of K_1 and K_2 from the statistical relationship for binary structures (Rubin, 1995): $\ln \bar{K}_{Z1} = (1-p) \cdot \ln K_1 + p \cdot \ln K_2$ and $\ln \bar{K}_{Z2} = p \cdot \ln K_1 + (1-p) \cdot \ln K_2$ using the mean conductivities of the zones $\bar{K}_{Z1} = 2e-6\,\mathrm{m/s}$ and $\bar{K}_{Z2} = 2e-4$. p is deduced from the flowmeter profiles (Figure 2a). Being from both zones Z_1 and Z_2, the profiles differ significantly in their average value. However, all show a tendencies of binary behavior with a significant spread over depth. The data is grouped into high and low values being at least two orders of magnitude apart. Then, p is the fraction of values in the minor group, which is $10-20\%$ for the MADE flowmeter profiles (Figure 2a) leading to $p = 15\%$ as default value.

The inclusions structure in both zones is design according to the simplified block structure outlined in paragraph 2.2. The domain is divided into horizontal blocks of length I_h. Each block contains randomly located inclusions of thickness I_v. The flowmeter logs at MADE indicate a change in vertical layering every $0.25-1\,\mathrm{m}$ (Figure 2a). Thus, we chose $I_v = 0.5\,\mathrm{m}$. In

270   combination with a inclusion percentage of $p = 15\%$ and an aquifer thickness of $10\,\mathrm{m}$ this gives three inclusions per block. We specify I_h through an heuristic approaches in combination with parametric uncertainty to rely on as little data as possible: The anisotropy ratio from the large scale pumping tests (Boggs et al., 1990)) is $e = 0.1 - 0.025$. Combining it with the inclusion thickness of $I_v = 0.5\,\mathrm{m}$ gives a range of $I_h \in [5\,m, 20\,m]$. Figure 5b shows an example structure for $I_h = 10$ m. Note that inclusion can touch, so some inclusions are thicker (e.g. $2I_v = 1$ m) and longer (e.g. $2I_h = 20$ m).

275   For our Monte Carlo Approach, we create ensembles of 600 individual random realizations. Allowing for parametric uncertainty, we consider three possible I_h values of 5 m, 10 m and 20 m when generating random realizations. The other parameters are fixed to the values outlined above. Reported flow and transport results for the inclusion structure in zones (A+B) are ensemble means. We checked for ensemble convergence and found that 200 realizations are already sufficient.

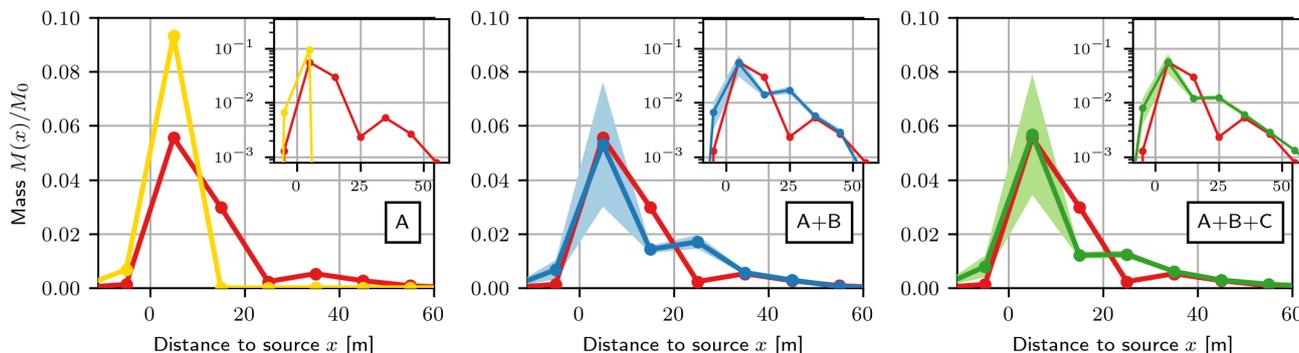### 3.2.3   Sub-scale Heterogeneity in Zones (A+B+C)

280   We combine modules (A), (B), and (C) to an inclusion structure in deterministic zones with small-scale fluctuations (A+B+C), depicted in Figure 5, bottom. Structural aspects of modules (A) and (B) are the same as described before, including parametric uncertainty for the inclusion length $I_h \in \{5, 10, 20\}$ m. Module C is integrated as log-normal distributed conductivity fluctuations (section 2.2). The characterizing parameters for Module (C) depend on the statistics of the super-ordinate modules (A) and (B).

285   The log-normal fluctuations $\ln Y(\boldsymbol{x})$ are generated with zero mean, since the overall mean conductivity refers to $\bar{K}_{Z1}$ and $\bar{K}_{Z2}$ of the deterministic zones. The log-conductivity variance σ_Y^2 follows from the "variance gap", as difference between the variance of the inclusion structure and the overall variance. The binary inclusions for the chosen setting have a variance of $\sigma_Z^2 = 5.52$ resulting from $\sigma_Z^2 = p \cdot (1-p) \cdot (\ln K_1 - \ln K_2)^2$ (Rubin, 1995). With an overall variance of $\sigma_F^2 = 5.9$ as indicated by (Bohling et al., 2016) (Figure 4), we arrive at a fluctuation variance of $\sigma_Y^2 \approx 0.5$. We apply an exponential co-variance
290   function with length scale parameters being a fraction of the inclusion length scales: $\lambda_h = 1/4 I_h$ and $\lambda_v = 1/4 I_v$. Testing several ratios, we saw that its impact on transport behavior is negligible. Ensembles consist of 600 realizations.

3.3   Numerical Model Settings

Flow and transport are calculated making use of the finite element solver OpenGeoSys (Kolditz et al., 2012) in the ogs5py python framework (Müller et al., 2020). The simulation domain is a 2D cross section within $x \in [-20, 200]$ m and $z \in [52, 62]$ m
295   generously comprising the area of the MADE-1 tracer experiment (Boggs et al., 1992). We applied constant head boundary conditions at the left and right margin with a mean had gradient of $J = 0.003$. Tracer is injected at a well located at $x = 0$ with a central screen of 0.6 m depth. Injection takes place over a period of $48.5\,\mathrm{h}$ with an injection rate of $Q_{in} = 1.166e - 5\,\mathrm{m^3/s}$ according to the initial conditions reported by Boggs et al. (1992). For technical details, the reader is referred to the *Supporting Information*.

300   Simulation results are processed like the MADE-1 experimental data. Longitudinal mass distributions are vertical averages and accumulated horizontally over $10\,\mathrm{m}$ slices. Note that the simulated distributions show a full mass recovery. Besides spatial

Figure 6. Longitudinal mass distribution at $T = 126$ days for conductivity concepts: (A) deterministic zones, (A+B) inclusions in zones, (A+B+C) inclusion in zones with sub-scale heterogeneity (Figure 5). Shaded areas (light blue and green) indicate parametric uncertainty bands. Mass distribution observed at MADE experiment in red. Linear scale and log-scale in subplot.

mass distributions for the six times where experimental data is available, we present the break through curves (BTCs) as temporal mass evolution at critical distances, although no BTCs data is reported for the MADE-1 experiment.

3.4 Simulation Results

305 Figure 6 shows the simulated longitudinal mass distributions $M(x)/M_0$ of the specified conductivity conceptualizations (section 3.2) at $T = 126$ days after injection. They are compared to the MADE-1 experiment data, which had a mass recovery of 99% at that time.

The mass distribution for the deterministic structure (concept A, yellow) shows a sharp peak close to the injection location and no mass downstream. The conductivity structures with inclusions in deterministic zones (A+B, blue) and with sub-scale

310 heterogeneity (A+B+C, green) result in skewed mass distributions with a peak close to the injection area and a small amount of mass ahead of the bulk. Shaded areas indicate parametric uncertainty due to the variable inclusion length I_h. The shade area margins refer to ± 3 ensemble standard deviations, which is similar to the 99% confidence intervals.

A direct comparison of the mass distributions $M(x)/M_0$ for the structures are depicted in Figure 7 for six temporal snapshots, including $T = 1000$d, where no experimental data is available. The general form of the mass distributions is persistent

315 in time for all conductivity structures.

Figure 8 shows simulated breakthrough curves (BTCs) for the deterministic block and inclusion conductivity structure at three distances to the injection location. The results for concept (A+B+C) are very close to those of concept (A+B), thus not displayed. Apparent differences to the longitudinal mass distributions as in Figure 7 are due to the spatial data aggregation. The BTC for Module A has the expected Gaussian shape with a late breakthrough at $x = 5$ m given the very low conductivity

320 in the injection area. The stochastic models have an earlier breakthrough and strong tailing at all distances.

13

Hydrology and
Earth System
Sciences
Discussions

EGU

Open Access
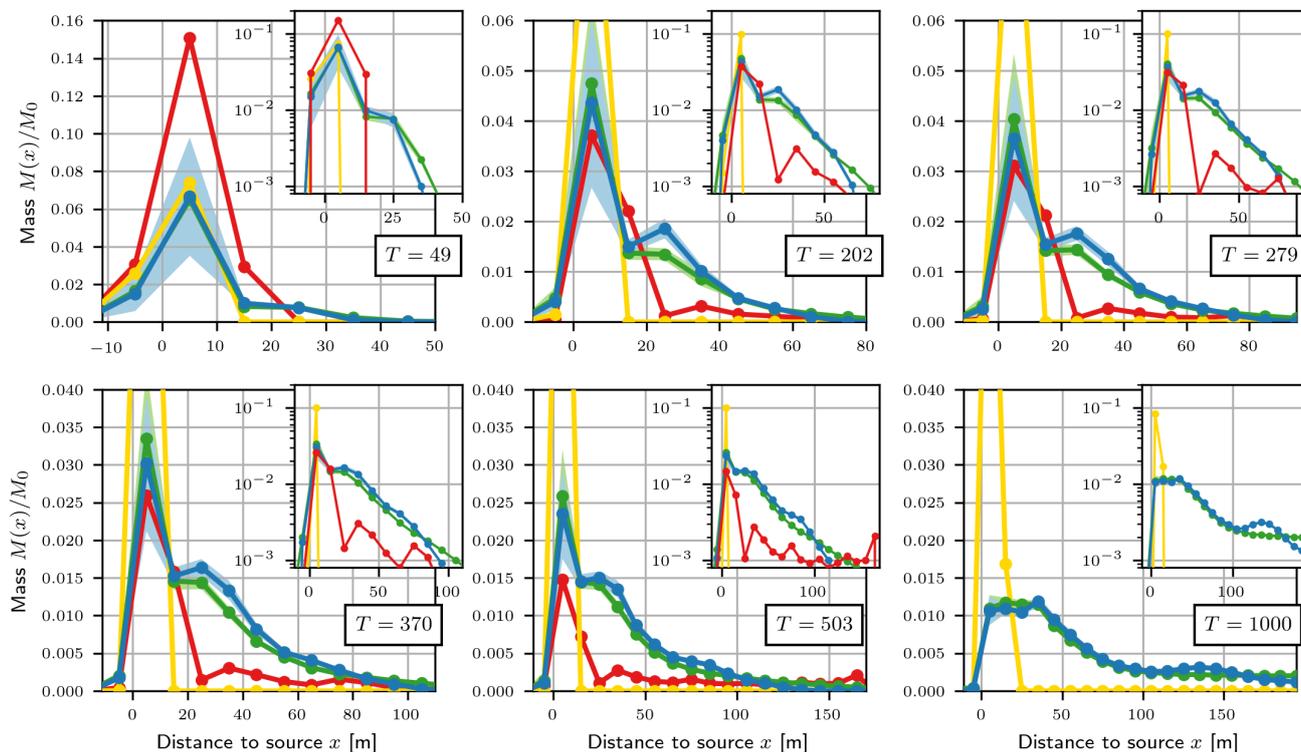
Figure 7. Mass distributions at times $T = 49, 202, 279, 370, 503$, and 1000 days (panels): red = MADE-1 experiment; yellow = concept (A); blue = concept (A+B); green = concept (A+B+C). Shaded areas (light blue and green) indicate parametric uncertainty bands; semi-log scale in subplot.

BTCs are not available for the MADE-1 transport experiment. However, we added the aggregated mass values at the three locations for the six reported times in a subplot to indicate a trend of temporal mass development. Note that mass values of the btcs and those at MADE are at different scales due to data aggregation and mass recovery.

3.5 Discussion

325   All conductivity structures were able to reproduce the skewed hydraulic head distribution as observed at MADE (Figure 1a). The corresponding mean flow velocity determines the travel time. As a results, all models properly reproduced the spatial position of the mass peak (Figure 6).

The deterministic block structure (A) failed to reproduce the skewed mass distribution observed at MADE. The leading front mass traveling through fast flow channels could not be predicted (Figure 7) solely using average K values in zones. In line
330   with model aim "Mean Arrival" (section 2.1), the simple structure allows to estimate the regional groundwater movement and
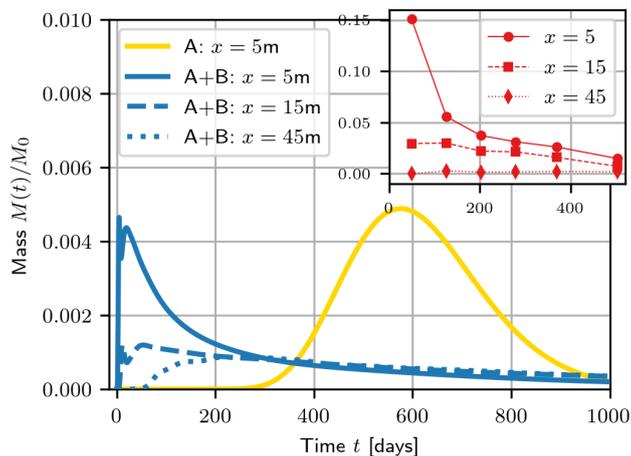
Figure 8. Breakthrough curves: Total mass $M(t)/M_0$ versus time at selected control plane locations for inclusion structure (A+B), (blue) at $x = 5$ m (solid), $x = 15$ m (dashed), $x = 45$ m (dotted); and for deterministic structure (A) at $x = 5$ m (solid yellow line). Reported mass values for MADE at the three locations (red markers) given in subplot. Regard the difference in scale due to the spatial averaging of experimental data.

to predict the location of the bulk mass. However, in case of aiming at "Risk Assessment", the arrival times of mass would be significantly underestimated, as clearly be observable comparing BTCs (Figure 8).

Tracer transport in a binary conductivity structure with inclusions (concept A+B) reproduces the observed mass, both for the peak near the injection site and the leading front. The simulated longitudinal mass distribution shows a second peak downstream
335 (Figure 7), which increases with time. The position is related to the interface between the low and high conductivity zones at 20 m distance to the source. Such a second peak is absent in the observed MADE-plume, however it might be associated with the mass loss for the later times. The skewed mass distribution is related to significantly smaller first arrival times as can be seen for the BTCs in Figure 8 compared to the deterministic structure. The BTCs are clearly non-Gaussian with heavy tailing. It shows the same temporal as the MADE experiment data.
340 The horizontal inclusion length I_h for structure (A+B) was not fixed, but was varied over the range of $I_h \in \{5, 10, 20\}$ m. The uncertainty bands in Figure 6b indicate that I_h mostly influences the height of the mass peak close to the source. I_h characterized the connectivity of the source area Z_1 to the high conductivity zone Z_2. Thus, it determines the distance of the bulk mass being trapped in the low conductivity area. The larger I_h the higher is the amount of mass transported downstream. The shape of the leading front is less impacted by I_h giving that its value does not influence the effect of the inclusions as
345 preferential flow per se.

The predicted plume shape for the conductivity structure with inclusions and subscale heterogeneity (A+B+C) is almost similar to the one without sub-scale heterogneity (A+B). consequently, the inclusion structure is the one which determines the

Hydrology and
Earth System
Sciences
Discussions
Open Access
EGU

shape of the distribution, whereas the impact of sub-scale heterogeneity is minor. Given the model aim of plume prediction, the additional effort for determining characterising geostatistical parameters for the sub-scale heterogeneity is not warranted.

350   The binary conductivity conceptualization (A+B) was derived for MADE with minimal data from field investigations, thus with a high parametric uncertainty. A sensitivity study revealed that the mass distribution resulting from the binary conductivity structure is very robust against the choice of parameters. The inclusion length I_h and the choice of the K contrast between the zones show the highest impact. The latter was expected as the mean conductivity determines the average flow velocity and by that the peak location and the general distribution shape. The impact of I_h is represented in the uncertainty bands (Figures 6b,

355   7). Other parameters as amount of inclusion p and sub-scale heterogeneity parameters as the variance have minor effects. For details, the reader is referred to the *Supporting Information*. In this regard, the binary structure is very stable towards parametric uncertainty.

4   Summary and Conclusions

We introduce a modular concept of heterogeneous hydraulic conductivity for predictive modeling of field scale subsurface

360   flow and transport. Central idea is to combine deterministic structures with simple stochastic approaches to rely on a minimal amount of measurements. The scale hierarchy of hydraulic conductivity induces three structure modules which represent: (A) deterministic large scale features like facies; (B) intermediate scale heterogeneity like preferential pathways or low conductivity inclusions; (C) small-scale random fluctuations. Field evidence of heterogeneity features and module's input parameters are provided by observation methods with the appropriate detection scale. The specific form of the scale-dependent features

365   depends on the site characteristics and field data. Generally, we propose a deterministic model for large-scale features, a simple binary statistical model for intermediate and a geostatistical model for small-scale features. However, the integration of alternative conductivity structures is possible.

An illustrative example is given for the heterogeneous MADE site. Three modular conductivity structures are constructed, based on two observations: (i) the existence of distinct zones of mean flow velocity, and (ii) high conductivity contrasts in

370   depth profiles suggesting local inclusions acting as fast flow channels. The structures are used in a predictive flow and transport model which is free of calibration. The comparison of results to the MADE-1 field tracer experiment showed that all conceptualizations can be of values depending on modelling aim. However, predicting the mass plume behaviour required to take heterogeneity into account.

The combination of deterministic and simple stochastic showed the best result given the trade-off between transport pre-

375   diction and need for measurements. Realizations of hydraulic conductivity composed of binary inclusions in two blocks with different average conductivity. Details on the topology are thereby secondary, since binary structures show robustness towards the choice of specific parameters. This rather simple structure was able to capture the overall characteristics of the MADE tracer plume with reasonable accuracy requiring only a small amount of observations. The generality of the concept makes it easily transferable to other sites; particularly when focusing on a few, but scale-related measurements.

380   A hierarchical conductivity structure allows to balance between complexity and available data. Large scale structures determine the mean flow behavior, which is most critical for flow predictions. They can be integrated to a model with reasonable low effort. Structural complexity increases with decreasing heterogeneity scale where small-scale features have the highest demand on observation data. However, even with limited information on the conductivity structure, simple stochastic modules can be used to incorporate the effect of heterogeneity. Considering small scale feature, the conductivity structure can be extended by
385 including modules when additional measurements are available.

Distinguishing the effects of the scale-specific features on flow and transport also allows to identify the need for further field investigations and potential strategies. The adaptive construction based on scale-specific modules allows to create a conductivity structure model as complex as necessary but as simple as possible.

The use of simple binary models is very powerful when dealing with strongly heterogeneous aquifers. They require less
390 observation data compared to uni-modal heterogeneity models, as log-normal conductivity with high variances. Binary models also allow to incorporate effects of dual-domain transport models without the drawback of having non-measurable input parameters which require model calibration. Our work shows that highly skewed solute plumes can be reproduced with classical ADE models by incorporating deterministic contrasts and effects of connectivity stochastically. specific transport analysis of less well investigated heterogeneous sites.

395   In summary, we conclude:

– When aquifer heterogeneity is at a similar scale as solute transport, predictive transport models need to incorporate spatially distributed hydraulic conductivity.

– Modular concepts of conductivity structure allow to separate the multiple scales of heterogeneity. Scale related investigation methods provide field evidence and characterizing model parameters. A hierarchical approach for conductivity
400   can thus minimize the effort by focusing on the model aim.

– Site specific heterogeneous hydraulic conductivity can be easily constructed with simple methods taking the (limited) amount of data into account. For aquifers with high conductivity contrast, we recommend combining large-scale deterministic structures and simple binary stochastics models.

– The application example at MADE showed that complex field structures can be represented appropriately for transport
405   predictions with an economic use of investigation data.

This work aims to contribute to bridging the gap between the advanced research in stochastic hydrogeology and its limited use by practitioners, being a subject of recent debate (e.g. Rajaram (2016)). We advocate the use of heterogeneity in transport models for successfully predicting solute behavior, particularly in complex aquifers. This can be done with few data and simple tools: adaptive structures allowing to combine deterministic, simple stochastic and geostatistical models depending on
410 the available data and the site-specific modelling aim.

Hydrology and
Earth System
Sciences
Discussions

Open Access

EGU

Code and data availability. Transport simulation and geo-statistical code used in this study is available on *https://github.com/GeoStat-Framework*. Data on the MADE aquifer can be accessed via the stated literature sources. Data generated for this study is available upon request to the corresponding author.

Author contributions. All authors contributed to developing the approach and writing the paper. Simulations and figure preparation was

415 performed by AZ.

Competing interests. No competing interests.

References

Adams, E. E. and Gelhar, L. W.: Field study of dipersion in a heterogeneous aquifer: 2. Spatial moments analysis, Water Resour. Res., 28, 3293–3307, https://doi.org/10.1029/92WR01757, 1992.

Bear, J.: Dynamics of Fluids in Porous Media, Elsevier, New York, 1972.

Boggs, J. M., Young, S., Benton, D., and Chung, Y.: Hydrogeologic Characterization of the MADE Site, Tech. Rep. EN-6915, EPRI, Palo Alto, CA, 1990.

Boggs, J. M., Young, S. C., Beard, L. M., Gelhar, L. W., Rehfeldt, K. R., and Adams, E. E.: Field study of dispersion in a heterogeneous aquifer: 1. Overview and site description, Water Resour. Res., 28, 3281–3291, https://doi.org/10.1029/92WR01756, 1992.

Bohling, G. C., Liu, G., Dietrich, P., and Butler, J. J.: Reassessing the MADE direct-push hydraulic conductivity data using a revised calibration procedure, Water Resour. Res., 52, 8970–8985, https://doi.org/10.1002/2016WR019008, 2016.

Carle, S. F. and Fogg, G. E.: Transition probability-based indicator geostatistics, Mathematical Geology, 28, 453–476, https://doi.org/10.1007/BF02083656, 1996.

Cirpka, O. A. and Valocchi, A. J.: Debates – Stochastic subsurface hydrology from theory to practice: Does stochastic subsurface hydrology help solving practical problems of contaminant hydrogeology?, Water Resour. Res., 52, 9218–9227, https://doi.org/10.1002/2016WR019087, 2016.

Dagan, G.: Flow and Transport on Porous Formations, Springer, New York, 1989.

Dietrich, P., Butler, J. J., and Faiss, K.: A rapid method for hydraulic profiling in unconsolidated formations, Ground Water, 46, 323–328, https://doi.org/10.1111/j.1745-6584.2007.00377.x, 2008.

Fetter, C. W.: Applied Hydrogeology, Prentice Hall, 2000.

Fiori, A.: Channeling, channel density and mass recovery in aquifer transport, with application to the MADE experiment, Water Resour. Res., 50, 9148–9161, https://doi.org/10.1002/2014WR015950, 2014.

Fiori, A., Dagan, G., Jankovic, I., and Zarlenga, A.: The plume spreading in the MADE transport experiment: Could it be predicted by stochastic models?, Water Resour. Res., 49, 2497–2507, https://doi.org/10.1002/wrcr.20128, 2013.

Fiori, A., Cvetkovic, V., Dagan, G., Attinger, S., Bellin, A., Dietrich, P., Zech, A., and Teutsch, G.: Debates – Stochastic subsurface hydrology from theory to practice: The relevance of stochastic subsurface hydrology to practical problems of contaminant transport and remediation. What is characterization and stochastic theory good for?, Water Resour. Res., 52, 9228–9234, https://doi.org/10.1002/2015WR017525, 2016.

Fiori, A., Zarlenga, A., Jankovic, I., and Dagan, G.: Solute transport in aquifers: The comeback of the advection dispersion equation and the First Order Approximation, Adv. Water Resour., 110, 349–359, https://doi.org/10.1016/j.advwatres.2017.10.025, 2017.

Fogg, G. E. and Zhang, Y.: Debates – Stochastic subsurface hydrology from theory to practice: A geologic perspective, Water Resour. Res., 52, 9235–9245, https://doi.org/10.1002/2016WR019699, 2016.

Fogg, G. E., Carle, S. F., and Green, C.: Connected-network paradigm for the alluvial aquifer system, Geological Society of America Special Papers, 348, 25–42, https://doi.org/10.1130/0-8137-2348-5.25, 2000.

Freeze, R. A.: A stochastic-conceptual analysis of the one-dimensional groundwater flow in nonuniform homogeneous media, Water Resour. Res., 11, 725–742, https://doi.org/10.1029/WR011i005p00725, 1975.

Gelhar, L.: Stochastic Subsurface Hydrology, Prentice Hall, Englewood Cliffs, N. Y., 1993.

Gomez-Hernandez, J., Butler, J. J., Fiori, A., Bolster, D., Cvetkovic, V., Dagan, G., and Hyndman, D.: Introduction to special section on
    Modeling highly heterogeneous aquifers: Lessons learned in the last 30 years from the MADE experiments and others, Water Resour.
    Res., 53, 2581–2584, https://doi.org/10.1002/2017WR020774, 2017.

Kitanidis, P.: Introduction to Geostatistics: Applications in Hydrogeology, Cambridge University Press, Cambridge ; New York, 2008.

Kolditz, O., Bauer, S., Bilke, L., Böttcher, N., Delfs, J.-O., Fischer, T., Görke, U. J., Kalbacher, T., Kosakowski, G., McDermott, C. I., Park,
    C. H., Radu, F., Rink, K., Shao, H., Shao, H. B., Sun, F., Sun, Y. Y., Singh, A. K., Taron, J., Walther, M., Wang, W., Watanabe, N., Wu, Y.,
    Xie, M., Xu, W., and Zehner, B.: OpenGeoSys: An open-source initiative for numerical simulation of thermo-hydro-mechanical/chemical
    (THM/C) processes in porous media, Environ. Earth Sci., 67, 589–599, https://doi.org/10.1007/s12665-012-1546-x, 2012.

Koltermann, C. E. and Gorelick, S. M.: Heterogeneity in Sedimentary Deposits: A Review of Structure-Imitating, Process-Imitating, and
    Descriptive Approaches, Water Resour. Res., 32, 2617–2658, https://doi.org/10.1029/96WR00025, 1996.

Kruseman, G. and de Ridder, N., eds.: Analysis and Evaluation of Pumping Test Data, ILRI publication, Wageningen, 47 edn., 2000.

Linde, N., Renard, P., Mukerji, T., and Caers, J.: Geological realism in hydrogeological and geophysical inverse modeling: A review, Adv.
    Water Resour., 86, 86–101, https://doi.org/10.1016/j.advwatres.2015.09.019, 2015.

Lu, Z. and Zhang, D.: On stochastic modeling of flow in multimodal heterogeneous formations, Water Resour. Res., 38, 1190,
    https://doi.org/10.1029/2001WR001026, 2002.

Müller, S., Zech, A., and Heße, F.: `ogs5py`: A Python-API for the OpenGeoSys 5 scientific modeling package, Ground Water, under
    revision, 2020.

Rajaram, H.: Debates – Stochastic subsurface hydrology from theory to practice: Introduction, Water Resour. Res., 52, 9215–9217,
    https://doi.org/10.1002/2016WR020066, 2016.

Rehfeldt, K. R., Hufschmied, P., Gelhar, L. W., and Schaefer, M.: Measuring hydraulic conductivity with the borehole flowmeter, Tech. Rep.
    EN-6511, EPRI, Palo Alto, CA, 1989.

Rehfeldt, K. R., Boggs, J. M., and Gelhar, L. W.: Field study of dispersion in a heterogeneous aquifer: 3. Geostatistical analysis of hydraulic
    conductivity, Water Resour. Res., 28, 3309–3324, https://doi.org/10.1029/92WR01758, 1992.

Renard, P., Straubhaar, J., Caers, J., and Mariethoz, G.: Conditioning Facies Simulations with Connectivity Data, Math Geosci., 43, 879–903,
    https://doi.org/10.1007/s11004-011-9363-4, 2011.

Rubin, Y.: Flow and Transport in Bimodal Heterogeneous Formations, Water Resour. Res., 31, 2461–2468,
    https://doi.org/10.1029/95WR01953, 1995.

Sanchez-Vila, X. and Fernàndez-Garcia, D.: Debates – Stochastic subsurface hydrology from theory to practice: Why stochastic modeling
    has not yet permeated into practitioners?, Water Resour. Res., 52, 9246–9258, https://doi.org/10.1002/2016WR019302, 2016.

Werth, C. J., Cirpka, O. A., and Grathwohl, P.: Enhanced mixing and reaction through flow focusing in heterogeneous porous media, Water
    Resour. Res., 42, W12 414, https://doi.org/10.1029/2005WR004511, 2006.

Zech, A. and Attinger, S.: Technical note: Analytical solution for the mean drawdown of steady state pumping tests in two-dimensional
    isotropic heterogeneous aquifers, Hydrol. Earth Syst. Sci. Discuss., 12, 6921–6944, https://doi.org/10.5194/hessd-12-6921-2015, 2015.

Zech, A., Müller, S., Mai, J., Heße, F., and Attinger, S.: Extending Theis' Solution: Using Transient Pumping Tests to Estimate Parameters
    of Aquifer Heterogeneity, Water Resour. Res., 52, 6156–6170, https://doi.org/10.1002/2015WR018509, 2016.

Zech, A., D'Angelo, C., Attinger, S., and Fiori, A.: Revisitation of the dipole tracer test for heterogeneous porous formations, Adv. Water
    Resour., 115, 198–206, https://doi.org/10.1016/j.advwatres.2018.03.006, 2018.

Zheng, C., Bianchi, M., and Gorelick, S. M.: Lessons Learned from 25 Years of Research at the MADE Site, Ground Water, 49, 649–662, https://doi.org/10.1111/j.1745-6584.2010.00753.x, 2011.

Zinn, B. and Harvey, C. F.: When good statistical models of aquifer heterogeneity go bad: A comparison of flow, dispersion, and mass transfer in connected and multivariate Gaussian hydraulic conductivity fields, Water Resour. Res., 39, 1051, 2003.